Hindawi
BioMed Research International
Volume 2018, Article ID 9873471, 16 pages
https://doi.org/10.1155/2018/9873471

Research Article

Dynamic Expression of Genes Involved in Proteoglycan/Glycosaminoglycan Metabolism during Skin Development

P. J. E. Uijtdewilligen,[1] **E. M. Versteeg**,[1] **E. M. A. van de Westerlo**,[1] **J. van der Vlag**,[2] **W. F. Daamen**,[1] **and T. H. van Kuppevelt**[1]

[1]*Department of Biochemistry, Radboud University Medical Center, Radboud Institute for Molecular Life Sciences, Nijmegen, Netherlands*
[2]*Department of Nephrology, Radboud University Medical Center, Radboud Institute for Molecular Life Sciences, Nijmegen, Netherlands*

Correspondence should be addressed to P. J. E. Uijtdewilligen; peterudw@gmail.com

Received 23 March 2018; Accepted 4 July 2018; Published 29 August 2018

Academic Editor: Kui Li

Glycosaminoglycans are important for cell signaling and therefore for proper embryonic development and adult homeostasis. Expressions of genes involved in proteoglycan/glycosaminoglycan (GAG) metabolism and of genes coding for growth factors known to bind GAGs were analyzed during skin development by microarray analysis and real time quantitative PCR. GAG related genes were organized in six categories based on their role in GAG homeostasis, *viz.* (1) production of precursor molecules, (2) production of core proteins, (3) synthesis of the linkage region, (4) polymerization, (5) modification, and (6) degradation of the GAG chain. In all categories highly dynamic up- and downregulations were observed during skin development, including differential expression of GAG modifying isoenzymes, core proteins, and growth factors. In two mice models, one overexpressing heparanase and one lacking C5 epimerase, differential expression of only few genes was observed. Data show that during skin development a highly dynamic and complex expression of GAG-associated genes occurs. This likely reflects quantitative and qualitative changes in GAGs/proteoglycans, including structural fine tuning, which may be correlated with growth factor handling.

1. Introduction

During various cell signaling processes, glycosaminoglycans (GAGs), such as heparan sulfate (HS), chondroitin sulfate (CS), and dermatan sulfate (DS), play a role in binding, guiding, and modulating signaling molecules, *e.g.*, growth factors and morphogens [1–3]. In skin this role can be illustrated by the importance of GAGs in adult wound healing [2, 4] and in the extracellular matrix architecture formed during dermal development [5, 6]. A further example to illustrate the importance of GAGs comes from mice overexpressing heparanase, an enzyme involved in the degradation of HS, showing accelerated hair growth [7], indicating its involvement in hair follicle morphogenesis and homeostasis. Other observations show that HS is involved in hair follicle cycling, sebaceous gland morphogenesis, and homeostasis [8]. Finally, HS and heparanase influence wound healing in adult mice by enhancing keratinocyte migration and stimulating blood vessel maturation [9]. Taken together, GAGs play an important role in skin healing and development and this prompted us to evaluate the expression of GAG related genes during (embryonic) development in skin.

Inhibition of the expression of genes coding for enzymes involved in GAG modification reactions clearly indicates the importance of GAGs during organogenesis [10], especially with respect to growth factor handling. For example, mice deficient in Ndst1 (N-deacetylase sulfotransferase isoenzyme 1) die neonatally due to several defects in which defective sonic hedgehog (Shh) signaling is implicated [11, 12]; mice deficient in Hs2st (heparan sulfate 2-O sulfotransferase) or Glce (glucuronic acid epimerase) display renal agenesis [13, 14], whereas mice deficient in Hs6st1 (heparan sulfate

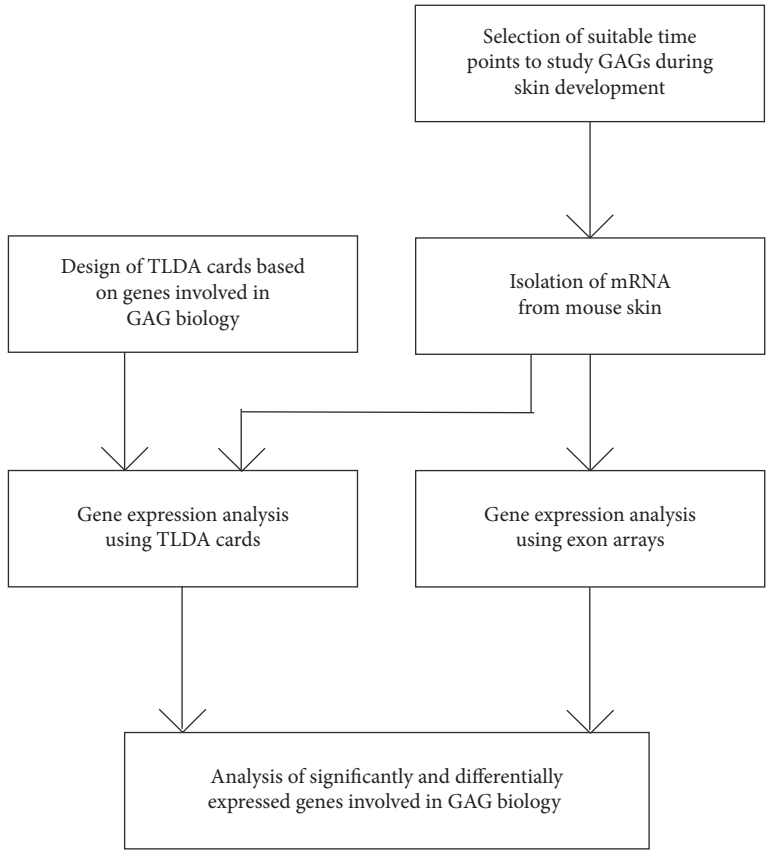

Figure 1: Experimental setup used for the analysis of gene expression involved in GAG biology during skin development in mice. Based on literature data, specific time points in skin development were selected. RNA was isolated, verified, and subsequently analyzed with GeneChip exon arrays and TLDA gene expression cards.

6-O sulfotransferase isozyme 1) show aberrant signaling of VEGF (vascular endothelial growth factor) and impaired lung development [15]. A skin phenotype of the above mouse models, however, has not been reported.

In general, it is thought that specific modifications of the GAG chain are involved in the binding and modulation of signaling molecules resulting in cell-type and/or tissue specific reactions [2, 3]. GAG mimetics like the RGTAs (regenerating agents) have been used to treat skin disorders and improve skin healing [16, 17]. To obtain insight in GAG metabolism during skin development we studied the expression of GAG related genes covering six functional classes ranging from the synthesis of precursor molecules to the synthesis and degradation of GAGs. In addition, we probed the expression of a number of (GAG binding) signaling molecules.

2. Materials and Methods

An overview of the experimental setup on the gene expression during murine skin development is given in Figure 1.

2.1. Animals for the Study on Skin Development. NIH guidelines for the care and use of laboratory animals (NIH publication 85–23 Rev. 1985) were followed. The study was approved by the Ethics Committee of the Radboud university medical center (DEC 2005-111, project: 81027). C57BL6/j mice were obtained from Elevage Janvier (Le Genest Saint Isle, France). Mice aged 90 days (90 days post birth [P90]) were used for timed mating and dorsal skin was collected at 14 days (E14) and 16 days after conception (E16). At E14 hair follicle development is initiated, and at E16 this process is almost completed in combination with a stratified epidermis and organized dermis [18, 19]. For the RNA samples of E14, dorsal skin of seven embryos from one female was pooled and used for RNA isolation. Skin was isolated at E14 by snap freezing the whole embryo in liquid nitrogen followed by scraping the skin layer in a cryomicrotome with a scalpel to minimize contamination with other embryonic tissues (skin is very thin at this time point). Samples were stored at -80°C. RNA samples for E16 were taken from two females, collecting dorsal skin form 7 embryos each. In addition, skin from 1-day old pups (P1) and adult mice (P90) was collected. At P1 skin is more organized and has been exposed to air [18, 19]. For the two dorsal skin samples for P1, three pups from two females were taken per sample. Two adult three-month old mice were used for the two dorsal skin samples at P90. Samples for RNA isolation for E16, P1, and P90 were collected by removing dorsal skin and snap freezing it in liquid nitrogen and storage at -80°C.

2.2. Tissue of Genetically Modified Mice. Skin samples of glucuronic acid epimerase (Glce) knockout mice (E18.5 for expression analysis; E17.5 and E18.5 for histological analysis) and of heparanase overexpression (Hpse) mice (P70) were provided by Prof. Dr. Jin-Ping Li (Department of Medical Biochemistry and Microbiology, University of Uppsala, Sweden) and Prof. Dr. Israel Vlodavsky (Vascular and Cancer Biology Research Center Rappaport Faculty of Medicine and Research Institute Technion-Israel Institute of Technology, Israel), respectively [7, 20]. For RNA isolation two wildtype and two mutant mice were used of both mouse models.

2.3. RNA Isolation, Real Time Quantitative PCR, and Microarray Analysis. Frozen samples were grinded in a microdismembrator (Sartorius, Bunnik, The Netherlands) and RNA was isolated using the TRIZOL-method (Invitrogen, Paisley, UK) in combination with RNeasy Mini kit with DNAse step (Qiagen, Hilden, Germany). RNA quality was assessed using the Bioanalyzer system (Agilent Technologies, Amstelveen, The Netherlands). The RNA integrity numbers (RIN, 27) were 8.8±0.25 (technical replicate N=2), 8.0±0.35, 8.5±0.55, and 7.3±0.2 for E14, E16, P1, and P90 (biological replicates N=2), respectively. The same procedure was used for the RNA isolation for the Glce knockout mouse and Hpse overexpression mouse. The RIN was 6.5±0.51 for *Glce*-/- samples and 8.0±0.48 for *Glce*+/+ and 6.3±0.3 and 7.7±0.6 for HPA-TG and HPA-WT, respectively (all biological replicate N=2).

Gene Chip Mouse exon 1.0 ST Arrays (Affymetrix, High Mycombe, UK) were used to analyze gene expression for E14, E16, P1, and P90 using 1 μg of RNA per chip. Expression data were preprocessed to check sensitivity and specificity of the results based on Kadota et al. (2009) as shown in Uijtdewilligen et al. (2016) [18, 21]. Gene level expression data were calculated for the CORE transcripts (probe sets supported by RefSeq mRNAs) using Affymetrix Expression Console software with quantile normalization (all arrays are considered to have an equal intensity distribution), GC-content background correction (probes with high GC-content hybridize better, corrected for with built-in probes with different known GC-contents) and summarization with the RMA algorithm [22]. Data were imported into GeneSpring GX 7.3 (Agilent Technologies), duplicates were averaged, and the expression of each transcript was normalized to the median per array.

Real Time-Quantitative PCR (qPCR) was performed using custom designed Taqman Low Density arrays (TLDA) (Applied Biosystems, Nieuwerkerk aan de IJssel, the Netherlands) containing probes against genes involved in GAG metabolism and GAG binding proteins (Supplementary data Table 1). Glce and Hpse samples were analyzed using qPCR using custom designed TLDA with an adapted design containing additional GAG related genes (Supplementary data Table 2).

For the TLDA cards, 100 ng cDNA in Taqman Universal PCR Master Mix (Applied Biosystems) was loaded on the TLDA card per slot and run on a 7900HT Fast Real Time PCR System (Applied Biosystems). Expression was analyzed based on the threshold cycle (Ct) which was obtained using the SDS 2.3 software and RQ Manager 1.2 of Applied Biosystems using the combined expression data of the tested TLDA cards. In Microsoft Excel the reference genes for ΔCt calculation were checked for stability of expression by analyzing the results of the reference genes across all used TLDA cards and selecting the reference genes with the smallest deviation across the cards tested. Subsequently ΔCt values were calculated using a reference gene with the smallest difference between the average Ct found for the gene of interest and for the reference gene. The obtained ΔCt values were further processed using the $2^{-\Delta\Delta Ct}$ method using P90 as a calibration point in case of the developmental study and the wild type background (C57BL6 mice) data in case of the two mouse models [23].

2.4. Statistical Methods. Statistical significance of the exon array data was analyzed using ANOVA and Benjamini-Hoghberg multiple testing correction [24]. Statistical significance of the TLDA card data was tested with an unpaired T-test (2-tailed) using Microsoft Excel. Data with a statistical threshold of $p<0.10$ and a fold threshold of >2.0 were considered statistically significant.

3. Results

Genes involved in glycosaminoglycan (GAG) synthesis, modification, and degradation were studied during skin development at 14 and **16 days** after **conception** (E14 and E16, respectively) and at one day after birth (P1) and compared to mature skin of a 3 month old mouse (P90). In addition, two mouse models, a Glce knockout mouse (E18.5) and an Hpse overexpression mouse model (P70), were analyzed. Taqman Low Density Array (TLDA) cards were designed to contain genes involved in GAG metabolism (Supplementary data Tables 1 and 2). The expression data obtained using TLDA cards and exon arrays were screened for genes with 2-fold differential expression at a statistical threshold of $p<0.10$ (Tables 1, 2, 3, and 4, Supplementary data Tables 4, 5, and 6).

In Tables 1–3 and Supplementary data Table 3, an overview is given of the differentially expressed genes applying TLDA cards and exon arrays. In all categories of genes involved in GAG metabolism, i.e., production of precursor molecules, core proteins, synthesis of linkage region, polymerization, modification and degradation of the GAG chain, and differences in expression were found (Tables 1–3). This indicates a highly dynamic expression pattern during skin development. Some isoenzymes were upregulated, whereas other isoenzymes were downregulated, further stressing metabolic complexity. This is, for instance, the case with GFPT1 and 2, both rates limiting enzymes involved in the production of hexosamines, and the isoenzymes HS 3-O sulfotransferase 6 and 3b1.

With respect to the core proteins, differential expression was found for both HS and CS/DS proteoglycans. Differential expression was found for two of the four syndecans, *viz. Sdc1* and *Sdc4*, three of the six glypicans, *viz. Gpc2, Gpc3*, and *Gpc6*, and *Hspg2* (Tables 2 and 3). The syndecans were downregulated, while the glypicans were upregulated, indicating an embryonic role for glypicans as described in literature

Table 1: Comparison of the number of differentially expressed genes during skin development in mice ($p<0.10$, fold>2.0) based on real-time qPCR and on exon array analysis.

Total genes	System	E14 vs. P90		E16 vs. P90		P1 vs. P90	
		Down	*Up*	*Down*	*Up*	*Down*	*Up*
Production of precursors							
43	TLDA	1	4	3	2	1	2
43	Exon	2	6	2	0	1	0
	Overlap	0	2	2	0	1	0
Core proteins							
14	TLDA	2	3	1	1	2	2
14	Exon	3	2	1	1	0	2
	Overlap	2	2	0	1	0	2
Preparation of linkage region							
8	TLDA	0	1	0	1	0	1
8	Exon	0	2	0	0	0	0
	Overlap	0	0	0	0	0	0
Glycosaminoglycan chain polymerisation							
13	TLDA	1	4	1	2	0	2
13	Exon	1	2	0	0	0	0
	Overlap	0	0	0	0	0	0
Glycosaminoglycan chain modification							
32	TLDA	1	9	0	5	0	8
32	Exon	1	3	0	3	0	1
	Overlap	1	2	0	1	0	0
Glycosaminoglycan chain degradation							
19	TLDA	2	2	3	1	0	1
19	Exon	3	1	1	1	2	0
	Overlap	2	1	1	1	0	0
Growth factors							
37	TLDA	0	13	3	8	1	11
37	Exon	2	14	3	10	1	4
	Overlap	0	10	2	8	0	4

∗ P values for the exon array measurements were calculated using Benjamini–Hochberg multitesting correction. P values for the TLDA assay were calculated using an unpaired T-test.
Overlap refers to genes differentially expressed in both TLDA card and exon array.

[25, 26]. *Hspg2*, a secreted HS presenting proteoglycan coding for perlecan [2], was found to be upregulated (Tables 2 and 3). Based on the exon array the CS/DS core protein of versican (Vcan) was upregulated at all time points (Supplementary data Table 5).

The upregulated expression of genes involved in the synthesis of the linkage region may signal increased GAG synthesis during development since after the formation of the linkage region the GAG chain is formed. For HS polymerization differential expression was found for, *e.g.*, *Extl1* and *Extl2*. *Extl1* showed downregulation at E14 while *Extl2* was upregulated, and both enzymes are involved in the initiation and elongation of the HS chain [2].

During and after synthesis of the glycosaminoglycan chain, disaccharide units within the chain are specifically modified. These modifications determine which effector molecules can bind to the chain and thus play a role in cell signaling [1, 3]. Upregulated expression was found for three of the four N-deacetylase/N-sulfotransferases (*Ndst*; TLDA cards, Table 2), especially isoenzyme *Ndst3*. Upregulation was also found for two out of seven genes coding for 3-O-sulfotransferases (*Hs3st1* and *Hs3st3b1*), involved in 3-O sulfation of GlcNS and GlnNAc residues, whereas one was downregulated (*Hs3st6)*.

The GlcNS and GlcNAc residues can also be 6-O sulfated by 6-O-sulfotransferases (Hs6st) [2] and selectively desulfated extracellularly by two sulfatases (*Sulf1* and *Sulf2*) aided by two cofactors (*Sumf1* and *Sumf2*) [2, 27]. *Hs6st2* was upregulated at all time points (Table 3). *Sulf1* was upregulated during embryonic development, whereas *Sumf2* was upregulated at E14 (Tables 2 and 3). These results indicate that specific expression of GAG modifying enzymes may play a role in specific cellular signaling during skin development.

Within the class of genes encoding for GAG chain degradation enzymes, two genes were differentially expressed. Heparanase expression was downregulated at E14 and P1 (Tables 2 and 3), whereas N-sulfoglucosamine sulfohydrolase

Table 2: Differentially expressed GAG related genes during skin development in mice in comparison to mature skin ($p<0.10$) based on real-time qPCR.

		E14 vs. P90		E16 vs. P90		P1 vs. P90	
Gene symbol	**Full gene name and probe set**	**P-value**	**Relative change**	**P-value**	**Relative change**	**P-value**	**Relative change**
Production of precursors							
Galk1 ‡	Galactokinase 1 Mm00444182_m1	***0.029***	***5.897***	***0.057***	***3.867***	***0.074***	***3.043***
Galt ‡	Gal-1-P-Uridylyltransferase Mm00489459_g1	*0.042*	*0.573*	***0.027***	***0.497***	0.832	0.964
Gfpt1 ‡	Glu-Fru-6-P-Transaminase 1 Mm00600127_m1	***0.002***	***2.378***	0.160	1.273	0.282	1.481
Gfpt2 ‡	Glu-Fru-6-P-Transaminase 2 Mm00496565_m1	0.269	0.772	***0.079***	***0.494***	0.356	0.780
Hk2 ‡	Hexokinase 2 Mm00443385_m1	*0.027*	*0.652*	0.253	1.390	*0.586*	*0.904*
Pgm3 ‡	Phosphoglucomutase 2 Mm00459270_m1	*0.058*	*1.876*	0.296	1.249	*0.098*	*1.470*
Pgm5 ‡	Phosphoglucomutase 5 Mm00723432_m1	***0.002***	***4.053***	***0.033***	***2.792***	***0.019***	***2.515***
Slc13a5 ‡	Solute Carrier Family 13 Member A5 Mm00523288_m1	Not detected		Not detected		Not detected	
Slc26a9 ‡	Solute Carrier Family 26 Member A9 Mm00628490_m1	Not detected		0.036	0.264	0.023	0.318
Slc35a3 ‡	Solute Carrier Family 35 Member a3 Mm00523288_m1	***0.008***	***0.444***	*0.060*	*0.567*	0.455	0.811
Core proteins							
Cd44	CD44 Molecule Mm01277164_m1	*0.018*	*0.536*	0.171	0.637	0.223	1.385
Gpc2 ‡	Glypican 2 Mm00549650_m1	***0.005***	***11.686***	0.638	1.294	0.369	1.249
Gpc3 †	Glypican 3 Mm00516722_m1	***<0.001***	***6.765***	***0.019***	***3.734***	***0.013***	***8.044***
Gpc6 ‡	Glypican 6 Mm00516235_m1	***0.027***	***2.880***	0.275	1.376	0.130	1.926
Hspg2 ‡	Perlecan Mm01181179_g1	*0.030*	*1.504*	*0.064*	*1.959*	***0.007***	***3.325***
Sdc1 ‡	Syndecan 1 Mm00448918_m1	***0.012***	***0.293***	0.107	0.313	***0.069***	***0.403***
Sdc4 †	Syndecan 4 Mm00488527_m1	***0.002***	***0.201***	***0.039***	***0.240***	***0.065***	***0.471***
Preparation of linkage region							
B3gat1	β-1,3-Glucuronyltransferase 1 Mm00661499_m1	Not detected		Not detected		Not detected	
B3gat2	β-1,3-Glucuronyltransferase 2 Mm00549042_m1	Not detected		Not detected		Not detected	
B4galt2 ‡	β-1,4-Galactosyltransferase 2 Mm00479556_m1	***0.023***	***4.562***	***0.059***	***2.679***	***0.038***	***3.384***
Glycosaminoglycan chain polymerisation							
Chpf ‡	Chondroitin Polymerizing Factor Mm01262239_g1	***<0.001***	***2.991***	*0.059*	*1.865*	***0.050***	***2.401***
Chsy1 ‡	CS Synthase 1 Mm01319178_m1	***0.013***	***3.900***	***0.024***	***2.282***	***0.072***	***2.229***
Chsy3 ‡	CS Synthase 3 Mm01545329_m1	***0.026***	***4.006***	***0.075***	***2.184***	0.101	2.013

Table 2: Continued.

Gene symbol	Full gene name and probe set	E14 vs. P90		E16 vs. P90		P1 vs. P90	
		P-value	Relative change	P-value	Relative change	P-value	Relative change
Csgalnact1 ‡	CS-GalNAc-transferase 1 Mm00555164_m1	***0.099***	***0.496***	***0.098***	***0.475***	0.634	1.128
Extl1 ‡	Exostoses (multiple)-like 1 Mm00621977_s1	Not detected		Not detected		Not detected	
Extl2 ‡	Exostoses (multiple)-like 2 Mm00469621_m1	***0.007***	***2.043***	0.660	1.220	0.106	1.765
Has2 ‡	Hyaluronan Synthase 2 Mm00515089_m1	0.188	1.933	0.235	1.705	0.410	1.577
Glycosaminoglycan chain modification							
Chst11 ‡	Chondroitin 4-O-Sulfotransferase 1 Mm00517563_m1	***0.002***	***3.000***	*0.087*	*1.195*	*0.087*	*1.957*
Chst14 ‡	Dermatan 4 Sulfotransferase 1 Mm00511291_s1	***0.026***	***2.459***	0.156	1.513	0.203	1.707
Chst2 ‡	Carbohydrate Sulfotransferase 2 Mm00490018_g1	***0.014***	***3.664***	***0.010***	***3.145***	***0.006***	***2.773***
Chst3 ‡	Chondroitin 6-O-Sulfotransferase 1 Mm00489736_m1	***0.041***	***3.241***	0.152	1.941	***0.028***	***3.550***
Chst8 ‡	GalNAc-4-O-Sulfotransferase 1 Mm00558321_m1	***0.089***	***2.587***	0.221	0.591	0.139	2.280
Hs3st1 ‡	HS 3-O-sulfotransferase Mm01964038_m1	*0.051*	*1.796*	*0.039*	*1.937*	***0.027***	***2.809***
Hs3st3b1‡	HS 3-O-sulfotransferase 3b1 Mm00479621_m1	***0.004***	***3.204***	***0.028***	***2.511***	***0.002***	***2.629***
Hs3st6 ‡	HS 3-O-sulfotransferase 6 Mm01299930_m1	***0.006***	***0.208***	*0.089*	*0.664*	*0.041*	*1.765*
Hs6st2	HS 6-O-sulfotransferase 2 Mm00479296_m1	Not detected		Not detected		Not detected	
Ndst1 ‡	N-deacet./N-sulfotrans. 1 Mm00447005_m1	0.118	1.487	0.140	1.449	***0.054***	***2.202***
Ndst2 ‡	N-deacet./N-sulfotrans. 2 Mm00447818_m1	*0.008*	*1.347*	***0.001***	***2.017***	***0.002***	***2.021***
Ndst3 ‡	N-deacet./N-sulfotrans. 3 Mm00453178_m1	***0.004***	***4.708***	***0.041***	***7.910***	***0.004***	***12.034***
Sulf1 ‡	Sulfatase 1 Mm00552283_m1	***0.004***	***4.644***	***0.079***	***2.674***	***0.089***	***2.077***
Sumf2 ‡	Sulfatase modifying factor 2 Mm01197721_m1	***0.008***	***2.657***	0.104	2.023	*0.038*	*1.857*
Glycosaminoglycan chain degradation							
ArsJ ‡	Arylsulfatase J Mm00557970_m1	***0.013***	***7.805***	***0.010***	***12.075***	***0.014***	***7.146***
ArsK ‡	Arylsulfatase K Mm00513099_m1	0.306	0.801	***0.059***	***0.466***	0.143	0.678
Galns ‡	Galactosamine (N-Acetyl)-6-Sulfatase Mm00489575_m1	<***0.001***	***2.648***	*0.066*	*1.674*	*0.091*	*1.584*
Hpse ‡	Heparanase Mm00461768_m1	***0.044***	***0.304***	0.342	1.450	0.169	0.578
Hyal1 ‡	Hyaluronoglucosamini-dase 1 Mm00476206_m1	***0.001***	***0.198***	***0.008***	***0.288***	*0.006*	*0.607*
Sgsh ‡	N-Sulfoglucosamine Sulfohydrolase Mm00450747_m1	*0.055*	*0.647*	***0.002***	***0.435***	0.644	0.897

Table 2: Continued.

Gene symbol	Full gene name and probe set	E14 vs. P90		E16 vs. P90		P1 vs. P90	
		P-value	Relative change	P-value	Relative change	P-value	Relative change
Growth factors							
Areg	Amphiregulin Mm00437583_m1	Not detected		Not detected		0.656	0.834
Bmp3 ‡	Bone morphogenetic growth factor 3 Mm00557790_m1	***0.007***	***4.270***	***0.004***	***7.240***	***0.002***	***11.628***
Bmp5 ‡	Bone morphogenetic growth factor 5 Mm00432091_m1	***0.022***	***12.051***	0.303	1.788	0.587	1.300
Ctgf ‡	Connective tissue growth factor Mm01192931_g1	0.668	1.079	***0.011***	***0.232***	*0.076*	*0.580*
Fgf10 ‡	Fibroblast growth factor 10 Mm00433275_m1	*0.063*	*1.649*	*0.050*	*1.801*	***0.093***	***2.262***
Fgf13 ‡	Fibroblast growth factor 13 Mm00438910_m1	***0.002***	***3.205***	*0.059*	*1.750*	0.181	1.544
Fgf2 ‡	Fibroblast growth factor 2 Mm01285715_m1	0.277	0.651	0.166	0.539	0.382	1.446
Fgf20	Fibroblast growth factor 20 Mm00748347_m1	Not detected		Not detected		Not detected	
Fgf22 ‡	Fibroblast growth factor 22 Mm00445749_m1	Not detected		0.386	0.632	*0.060*	*0.614*
Fgf7 ‡	Fibroblast growth factor 7 Mm00433291_m1	*0.045*	*0.606*	***0.002***	***0.394***	*0.087*	*0.630*
Fgf8	Fibroblast growth factor 8 Mm00438921_m1	Not detected		Not detected		Not detected	
Figf ‡	C-fos induced growth factor Mm01131929_m1	*0.081*	*1.397*	*0.030*	*1.787*	0.545	0.834
Gdf10 ‡	Growth differentaition factor 10 Mm03024279_s1	***0.015***	***3.181***	0.454	1.143	0.166	1.519
Hbegf ‡	Heparin-binding epidermal growth factor Mm00439305_g1	Not detected		***0.015***	***0.347***	***0.016***	***0.423***
Hdgf †	Hepatoma-derived growth factor Mm00725733_s1	0.257	1.221	0.737	0.911	0.975	1.008
Igf1 ‡	Insulin-like growth factor 1 Mm00439560_m1	0.320	1.207	0.217	0.705	0.364	0.790
Igf2 †	Insulin-like growth factor 2 Mm00439565_g1	***<0.001***	***592.335***	***0.002***	***338.094***	***0.001***	***416.096***
Nog ‡	Noggin Mm01297833_s1	***0.054***	***2.945***	***0.019***	***2.935***	***0.021***	***3.067***
Pdgfa ‡	Platelet-derived growth factor a Mm01205760_m1	***0.021***	***3.005***	Not detected		***0.016***	***3.669***
Pdgfb ‡	Platelet-derived growth factor b Mm01298578_m1	0.321	1.098	*0.033*	*1.468*	***0.010***	***2.096***
Pdgfc ‡	Platelet-derived growth factor c Mm00480205_m1	Not detected		***0.016***	***2.362***	Not detected	
Pdgfd ‡	Platelet-derived growth factor d Mm00546829_m1	Not detected		0.288	0.709	0.139	1.644
Shh	Sonic hedgehog Mm00436527_m1	Not detected		Not detected		Not detected	
Tgfb1 ‡	Transforming growth factor beta 1 Mm01178820_m1	*0.027*	*0.540*	0.488	0.817	0.157	1.372

Table 2: Continued.

Gene symbol	Full gene name and probe set	E14 vs. P90		E16 vs. P90		P1 vs. P90	
		P-value	Relative change	P-value	Relative change	P-value	Relative change
Tgfb2 ‡	Transforming growth factor beta 2 Mm01321739_m1	***0.039***	***2.697***	0.757	1.081	0.127	1.809
Tgfb3 ‡	Transforming growth factor beta 3 Mm01307950_m1	***0.033***	***2.420***	*0.094*	*1.854*	***0.034***	***2.517***
Vegfa ‡	Vascular endothelial growth factor a Mm01281447_m1	0.394	1.108	0.112	1.613	0.461	1.358
Vegfb	Vascular endothelial growth factor b Mm00442102_m1	Not detected		Not detected		Not detected	
Vegfc ‡	Vascular endothelial growth factor c Mm00437313_m1	*0.024*	*1.839*	0.303	1.250	*0.015*	*1.996*
Wnt10b ‡	Wingless-related integration site 10b Mm00442104_m1	0.180	5.829	0.122	9.688	0.105	11.748
Wnt16 ‡	Wingless-related integration site 16 Mm00446420_m1	***0.066***	***2.094***	***0.016***	***4.809***	***0.014***	***4.362***
Wnt2 ‡	Wingless-related integration site 2 Mm00470018_m1	***0.054***	***3.144***	*0.090*	*3.555*	*0.074*	*3.760*
Wnt2b	Wingless-related integration site 2b Mm00437330_m1	Not detected		Not detected		Not detected	
Wnt3a ‡	Wingless-related integration site 3a Mm00437337_m1	0.394	1.610	0.441	1.520	0.840	1.106
Wnt6 ‡	Wingless-related integration site 6 Mm00437353_m1	***0.015***	***11.709***	***0.018***	***10.400***	***0.016***	***10.758***
Wnt7a	Wingless-related integration site 7a Mm00437355_m1	Not detected		Not detected		Not detected	
Wnt7b ‡	Wingless-related integration site 7b Mm00437357_m1	***0.003***	***4.180***	***0.056***	***6.076***	***0.003***	***4.181***

Numbers in italic are significant ($p<0.10$); numbers in bold are >2-fold differentially expressed. Gene symbols indicated with a †-symbol are normalized using GAPDH as a reference gene. Gene symbols indicated with a ‡-symbol are normalized using TBP as a reference gene. Genes, for which a signal was not or only partly detected at a given time point or multiple time points and therefore a fold change and/or p value could not be calculated based on the available data, are given as "not detected." Gene symbols for which all time points were classified as "not detected" do not show a symbol for the used reference gene due to lack of data for a calculation.

(*Sgsh*) was downregulated during embryonic development at E16 (Table 2) and at E14 (Table 3).

In addition to genes involved in GAG metabolism, the TLDA card contained 37 genes encoding growth factors, which were also present in the microarray (Tables 2 and 3). Differential expression was found by both TLDA card and microarray analysis for 10, 9 and 4 growth factors at E14, E16 and P1 respectively. Examples are insulin-like growth factor 2 *(Igf2*), wingless-related integration site 6 (*Wnt6*), and *Wnt7b*. *Igf2* was dramatically upregulated at all time points, as expected based on previous research [18]. *Wnt6* was also upregulated at all time points, while *Wnt7b* was upregulated only during embryonic development.

Next to their expression during development, gene expression of GAG-associated genes was studied in a *Glce* (glucuronyl epimerase) knockout mouse model and a heparanase overexpression mouse model using TLDA cards. In the *Glce* knockout mice six genes were differentially expressed (Table 4). Three of them are involved in CS and DS proteoglycans and were downregulated, *i.e.*, aggrecan (*Acan*), asporin (*Aspn*), and chondroitin sulfate N-acetylgalactosaminyltransferase 2 (*Csgalnact2*). Up/downregulation was not found for HS related genes, except for *Glce*, which was downregulated as expected. For the heparanase overexpression mouse model, in which a human heparanase was overexpressed [7], the results showed only one gene to be differentially expressed, i.e., aggrecan *(Acan)* which was 2.5-fold upregulated. The complete results of both the *Glce* knockout mouse and the Hpse overexpression mouse are given in Supplementary data Table 6.

4. Discussion

GAGs play a regulating role during embryonic development of various organs [1–3]. Therefore, we examined the expression of genes involved in GAG metabolism during skin development using custom designed Taqman Low Density Arrays (TLDA card) and exon arrays. To structure the data we studied gene expression in six functional classes, *viz.* the production of precursor molecules, the synthesis

Table 3: Differentially expressed GAG related genes during skin development in mice in comparison to mature skin ($p<0.10$) based on gene Chip Mouse Exon 1.0 ST Arrays.

Gene symbol	Full gene name and probe set	E14 vs. P90		E16 vs. P90		P1 vs. P90	
		Stepup P-value	Fold change	Stepup P-value	Fold change	Stepup P-value	Fold change
Production of precursors							
Galk1	Galactokinase 1 6792485	***0.030***	***4.242***	0.126	2.483	0.231	2.194
Galt	Gal-1-P-Uridylyltransferase 6912944	0.664	0.814	0.231	1.864	0.665	1.340
Gfpt1	Glu-Fru-6-P-Transaminase 1 6947679	***0.020***	***2.110***	0.077	1.682	0.801	1.081
Gfpt2	Glu-Fru-6-P-Transaminase 2 6780767	0.176	0.610	***0.087***	***0.426***	0.229	0.547
Hk2	Hexokinase 2 6954982	***0.003***	***0.451***	*0.040*	*1.375*	*0.039*	*0.655*
Pgm3	Phosphoglucomutase 2 6997513	***0.083***	***2.193***	0.676	1.178	*0.654*	*1.286*
Pgm5	Phosphoglucomutase 5 6872290	***0.058***	***2.338***	***0.104***	***2.209***	***0.291***	***1.696***
Slc13a5	Solute Carrier Family 13 Member A5 6789531	***0.003***	***2.588***	*0.059*	*1.322*	0.576	1.075
Slc26a9	Solute Carrier Family 26 Member A9 6753079	**0.012**	**0.227**	***0.090***	***0.471***	***0.091***	***0.392***
Slc35a3	Solute Carrier Family 35 Member A3 6908510	0.105	0.767	*0.596*	*0.925*	0.572	0.890
Core proteins							
Cd44	CD44 Molecule 6889258	***0.009***	***0.370***	0.144	0.728	0.873	0.955
Gpc2	Glypican 2	Not measured		Not measured		Not measured	
Gpc3	Glypican 3 7016826	***0.003***	***4.339***	***0.013***	***3.305***	***0.015***	***4.721***
Gpc6	Glypican 6 6821985	***0.019***	***2.767***	0.109	1.747	0.193	1.640
Hspg2	Perlecan 6917933	0.309	1.183	*0.075*	*1.554*	***0.042***	***2.230***
Sdc1	Syndecan 1 6793226	***0.031***	***0.380***	***0.067***	***0.413***	0.103	0.424
Sdc4	Syndecan 4 6892905	***0.017***	***0.341***	*0.094*	*0.536*	0.215	0.621
Preparation of linkage region							
B3gat1	β-1,3-Glucuronyltransferase 1 6987632	***0.008***	***3.467***	0.256	1.302	0.828	0.929
B3gat2	β-1,3-Glucuronyltransferase 2 6748174	***0.009***	***3.241***	0.286	1.269	0.690	1.129
B4galt2	β-1,4-Galactosyltransferase 2 6924869	*0.039*	*1.726*	*0.053*	*1.856*	0.176	1.477
Glycosaminoglycan chain polymerisation							
Chpf	Chondroitin Polymerizing Factor 6759816	*0.071*	*1.679*	0.182	1.459	0.309	1.403

Table 3: Continued.

Gene symbol	Full gene name and probe set	E14 vs. P90		E16 vs. P90		P1 vs. P90	
		Stepup P-value	Fold change	Stepup P-value	Fold change	Stepup P-value	Fold change
Chsy1	CS Synthase 1	Not measured		Not measured		Not measured	
Chsy3	CS Synthase 3 6861281	0.429	1.153	*0.056*	*1.769*	0.849	1.058
Cs-galnact1	CS-GalNAc-transferase 1 6983073	0.137	0.512	0.202	0.541	0.974	0.975
Extl1	Exostoses (multiple)-like 1 6926017	***0.025***	***0.407***	0.149	0.625	0.144	0.505
Extl2	Exostoses (multiple)-like 2 6900659	*0.085*	*1.702*	0.819	1.066	0.518	1.272
Has2	Hyaluronan Synthase 2 6854042	***0.095***	***2.107***	0.157	1.969	0.537	1.403
Glycosaminoglycan chain modification							
Chst11	Chondroitin 4-O-Sulfotransferase 1 6769366	*0.049*	*1.922*	0.465	1.208	*0.239*	*1.531*
Chst14	Dermatan 4 Sulfotransferase 1 6880476	0.151	1.491	0.506	1.191	0.773	1.122
Chst2	Carbohydrate Sulfotransferase 2 6997990	***0.035***	***2.302***	***0.072***	***2.160***	0.207	1.682
Chst3	Chondroitin 6-O-Sulfotransferase 1 6774295	0.885	1.034	0.108	1.545	0.162	1.530
Chst8	GalNAc-4-O-Sulfotransferase 1 6966453	0.945	1.007	0.569	1.054	0.420	1.108
Hs3st1	HS 3-O-sulfotransferase 1 6937654	*0.074*	*1.658*	0.105	1.688	0.119	1.824
Hs3st3b1	HS 3-O-sulfotransferase 3b1 6788991	0.683	1.178	0.253	1.634	0.511	1.432
Hs3st6	HS 3-O-sulfotransferase 6 6849317	***0.019***	***0.406***	0.291	0.771	0.721	1.130
Hs6st2	HS 6O-sulfotransferase 2 7016808	***0.004***	***6.417***	***0.012***	***5.609***	***0.041***	***3.080***
Ndst1	N-Deacetylase and N-Sulfotransferase 1 6865926	*0.090*	*1.363*	*0.056*	*1.649*	*0.067*	*1.763*
Ndst2	N-Deacetylase and N-Sulfotransferase 2 6823122	0.822	1.044	*0.059*	*1.697*	*0.083*	*1.733*
Ndst3	N-Deacetylase and N-Sulfotransferase 3 6908958	0.173	2.472	0.111	3.856	0.122	4.860
Sulf1	Sulfatase 1 6747641	***0.010***	***4.522***	***0.051***	***2.546***	0.232	1.627
Sumf2	Sulfatase modifying factor 2	Not measured		Not measured		Not measured	
Glycosaminoglycan chain degradation							
ArsJ	Arylsulfatase J 6901136	***0.003***	***2.498***	***0.006***	***3.164***	*0.031*	*1.702*
ArsK	Arylsulfatase K 6814451	0.368	0.784	0.102	0.543	0.514	0.779
Galns	Galactosamine (N-Acetyl)-6-Sulfatase 6985943	*0.087*	*1.671*	0.322	1.311	0.786	1.115

Table 3: Continued.

Gene symbol	Full gene name and probe set	E14 vs. P90		E16 vs. P90		P1 vs. P90	
		Stepup P-value	Fold change	Stepup P-value	Fold change	Stepup P-value	Fold change
Hpse	Heparanase 6940363	***0.021***	***0.267***	0.540	1.244	***0.095***	***0.360***
Hyal1	Hyaluronoglucosamini-dase 1 6992224	***0.003***	***0.154***	***0.011***	***0.222***	***0.041***	***0.402***
Sgsh	N-Sulfoglucosamine Sulfohydrolase 6792702	***0.017***	***0.458***	*0.052*	*0.537*	0.201	0.699
Growth factors							
Areg	Amphiregulin 6932394	***0.016***	***0.157***	***0.043***	***0.200***	0.333	0.550
Bmp3	Bone morphogenetic growth factor 3 6932718	0.280	1.392	***0.067***	***2.381***	0.100	2.365
Bmp5	Bone Morphogenetic growth factor 5 6990569	***0.001***	***7.247***	0.141	1.191	0.688	1.057
Ctgf	Connective tissue growth factor 6766623	0.148	0.729	***0.025***	***0.366***	***0.068***	***0.485***
Fgf10	Fibroblast growth factor 10 6810592	0.138	1.521	***0.057***	***2.250***	***0.094***	***2.142***
Fgf13	Fibroblast growth factor 13 7017134	***0.012***	***2.998***	*0.075*	*1.824*	0.296	1.391
Fgf2	Fibroblast growth factor 2 6896850	0.201	0.664	0.279	0.696	0.952	0.967
Fgf20	Fibroblast growth factor 20 6981854	0.659	1.228	0.125	2.483	0.777	1.220
Fgf22	Fibroblast growth factor 22 6769141	***0.005***	***0.329***	0.972	0.994	*0.097*	*0.646*
Fgf7	Fibroblast growth factor 7 6880900	0.531	0.740	***0.078***	***0.286***	0.212	0.418
Fgf8	Fibroblast growth factor 8 6873363	0.492	0.883	0.655	1.085	0.682	0.895
Figf	C-fos induced growth factor 7015007	*0.051*	*1.734*	*0.062*	*1.909*	0.548	0.832
Gdf10	Growth differentiation factor 10 6818153	***0.028***	***2.334***	0.757	1.086	0.894	1.060
Hbegf	Heparin-binding epidermal growth factor 6864680	*0.037*	*0.551*	*0.063*	*0.547*	*0.087*	*0.530*
Hdgf	Hepatoma-derived growth factor 6899028	0.104	1.246	0.575	1.070	0.409	1.147
Igf1	Insulin-like growth factor 1 6769597	0.235	0.631	0.173	0.537	0.398	0.641
Igf2	Insulin-like growth factor 2 6972317	***0.001***	***59.615***	***0.002***	***55.864***	***0.002***	***52.364***
Nog	Noggin 6790670	0.275	2.605	0.517	1.773	0.677	1.712
Pdgfa	Platelet-derived growth factor a 6942654	***0.028***	***2.013***	***0.035***	***2.347***	***0.057***	***2.338***
Pdgfb	Platelet-derived growth factor b 6837144	*0.037*	*0.704*	0.199	1.197	0.157	1.298

Table 3: Continued.

Gene symbol	Full gene name and probe set	E14 vs. P90		E16 vs. P90		P1 vs. P90	
		Stepup P-value	Fold change	Stepup P-value	Fold change	Stepup P-value	Fold change
Pdgfc	Platelet-derived growth factor c 6898686	***0.019***	***2.152***	***0.035***	***2.207***	0.902	1.042
Pdgfd	Platelet-derived growth factor d 6986677	0.925	0.952	0.191	0.504	0.790	1.205
Shh	Sonic hedgehog 6936889	0.448	0.595	0.308	2.117	0.152	4.571
Tgfb1	Transforming growht factor beta 1 6959236	0.106	0.552	0.241	0.653	0.975	0.981
Tgfb2	Transforming growht factor beta 2 6764953	***0.057***	***2.441***	0.448	1.335	0.264	1.802
Tgfb3	Transforming growth factor beta 3 6802449	***0.026***	***2.386***	0.238	1.408	0.100	2.077
Vegfa	Vascular endothelial growth factor a 6855659	0.779	0.875	0.721	1.174	0.940	1.061
Vegfb	Vascular endothelial growth factor b 6871273	*0.008*	*1.461*	*0.031*	*1.318*	*0.060*	*1.277*
Vegfc	Vascular endothelial growth factor c 6976200	***0.088***	***2.120***	0.477	1.316	0.316	1.700
Wnt10b	Wingless-related integration site 10b 6838399	0.629	1.280	0.120	2.812	0.240	2.325
Wnt16	Wingless-related integration site 16 6944581	0.358	1.180	***0.026***	***2.402***	*0.093*	*1.710*
Wnt2	Wingless-related integration site 2 6951974	***0.057***	***3.047***	***0.082***	***3.260***	0.122	3.219
Wnt2b	Wingless-related integration site 2b 6907887	***0.009***	***2.189***	***0.024***	***2.030***	*0.077*	*1.590*
Wnt3a	Wingless-related integration site 3a 6788662	0.457	1.199	0.103	1.728	0.684	1.159
Wnt6	Wingless-related integration site 6 6750567	***0.011***	***3.166***	***0.032***	***2.668***	***0.064***	***2.352***
Wnt7a	Wingless-related integration site 7a 6955539	***0.060***	***2.117***	0.131	1.865	0.395	1.456
Wnt7b	Wingless-related integration site 7b 6837582	***0.072***	***2.297***	***0.050***	***3.623***	0.237	1.912

Numbers in Italic are significant ($p<0.10$); numbers in bold are >2-fold differentially expressed. Genes indicated as "not measured" represent genes for which probes were not available on the used exon array version.

of core proteins and the linkage region, and the synthesis, modification, and degradation of the GAG chain proper. In addition we studied a number of growth factors, since GAGs are involved in their regulation including growth factor diffusion and signaling [3, 28].

With respect to core proteins, the heparan sulfate proteoglycans syndecan and glypican showed notable differential expression (Tables 2 and 3). Glypicans play an important role in development and cell signaling [12, 26, 29], and we found upregulation of 3 out of 6 glypican core proteins. *Gpc3* was upregulated during embryonic development and one day postbirth, suggesting that this glypican has a role during skin development. A possible function of *Gpc3* in skin has been suggested for the *Gpc3*-null mouse, which showed pigmentation defects [30]. Humans deficient in *Gpc3* suffer from the Simpson-Golabi-Behmel syndrome (SBGS). Based on the symptoms of SGBS and the phenotype found for the *Gpc3*-null mice, it has been suggested that Gpc3 is involved in the regulation of hedgehog signaling [31], a signaling pathway involved in hair follicle development [32]. Surprisingly, the *Gpc3*-null mice did not show a defect in appendage formation [30], indicating a functional but not essential role. Further

Table 4: Differentially expressed genes in C5 epimerase (Glce) knockout mouse ($p<0.10$) based on real-time qPCR.

Gene symbol	Full gene name and probe set	P-value	Relative change
Production of precursors			
Gnpnat1	Glucosamine-Phosphate N-Acetyltransferase 1 Mm00834602_mH	***0.033***	***0.468***
Slc2a4	Solute Carrier Family 2 Member 4 Mm01245507_g1	***0.086***	***2.526***
Core proteins			
Acan	Aggrecan Mm00545807_m1	***0.005***	***0.242***
Aspn	Asporin Mm00445945_m1	***0.010***	***0.382***
Glycosaminoglycan chain polymerisation			
Csgalnact 2	CS N-Acetylgalactosaminyltransferase 2 Mm00513340_m1	***0.049***	***0.431***
Glycosaminoglycan chain modification			
Glce	Glucuronic Acid Epimerase Mm00473667_m1	***0.013***	***0.079***

Numbers in Italic are significant ($p<0.10$); numbers in bold are >2 fold differentially expressed.
All genes were normalized using 18S RNA as a reference gene.

research is needed to elucidate the role of *Gpc3* and the two other differentially expressed glypicans, *i.e., Gpc2* and *Gpc6*.

Syndecans are described to take part in adult wound healing [33]. We found downregulation of the core proteins of two syndecans during embryonic development, which could indicate that these proteoglycans do not play a major general role during skin development. Specific roles, such as the involvement of *Sdc1* in hair follicle development, as described on basis of immunohistochemical data [34], can, however, not be excluded.

In the class of GAG chain polymerization, we found differential expression of genes encoding for the initiation of HS or CS/DS synthesis. HS chain polymerization is initiated by the addition of GlcNAc by *Extl2* [35] or *Extl3* [36], while CS/DS chain polymerization is initiated by the addition of GalNAc by *Csgalnact1* [37]. *Extl2* was upregulated during early skin development (Table 2), while *Csgalnact1* was downregulated (Supplementary data Table 5), which suggests that during early skin development HS production is stimulated in comparison to CS/DS production.

Enzyme mediated chemical modifications of the GAG chains result in the creation of specific binding sites for effector molecules [38]. Enzymes forming the class of N-deacetylase/sulfotransferases (Ndst's) are initiating elements in this respect. Especially *Ndst3* was upregulated, being one of four enzymes responsible for the removal of the acetyl group from the N-acetylated glycosamine and for the addition of a sulfate group. The additional expression of *Ndst3* in combination with *Ndst1* and *Ndst2* points to the fine tuning of HS chains for specific recognition of ligands. *Ndst3* has a higher deacetylation activity in comparison to the N-sulfotransferase activity, while *Ndst1* and *Ndst2* have a slightly higher N-sulfotransferase activity [39]. In addition, the data on the expression of heparan sulfate 3-O sulfotransferases (Hs3sts) [40] and heparan sulfate 6-O-sulfotransferases (Hs6sts) [41] suggest dynamic and specific modification of HS chains.

Three genes encoding for enzymes involved in HS and CS/DS degradation were differentially expressed, one of them being *Hpse* (heparanase). *Hpse* is downregulated at E14 and at P1, but not at E16 at which time point hair follicle development is taking place. *Hpse* has been reported to be involved in this process [42, 43].

Glycosaminoglycans are involved in growth factor regulation during developmental processes [1, 2]. We therefore studied 37 growth factors implied in skin development. A number of genes encoding growth factors were differentially expressed during development and the data are in line with earlier results for, e.g., *Igf2* [18], *Wnt6*, and *Wnt7b* [44]. Although speculative, the dynamics in GAG structure may be correlated with the dynamics of growth factors.

Next to skin development we also studied gene expression in skin of a *Glce* (glucuronyl epimerase) knockout mouse and an Hpse (heparanase) overexpression mouse [7, 13]. In the *Glce* knockout mice relatively few genes were differentially expressed, suggesting that skin is relatively unaffected by the lack of *Glce* in line with the observation that skin in these mice is phenotypically normal [20]. The skin phenotype of the Hpse overexpression mouse shows accelerated hair growth [7]. Gene expression analysis of this model showed only one differentially expressed gene (aggrecan). These results may touch upon the regulation of translation of mRNAs coding for GAG related enzymes. Enzymes involved in the synthesis and modification of GAGs as well genes coding for (some) growth factors share a common alternative translation mechanism via IRES sites [45, 46]. In general mRNAs are translated by the ribosomal scanning mechanism which scans for short leader sequences of 50 to 70 nucleotides [46, 47]. The leader sequences of the HS modifying enzymes and growth factors are characterized by long but structured sequences, which

are not recognized by the ribosomal scanning mechanism [46, 47]. Within these sequences internal ribosomal entry sites (IRES) allow alternative translation, e.g., under stress conditions [47]. This indicates that in addition to mRNA levels an additional control mechanism on the translational level may be present. In addition, other types of regulatory levels are known including the interaction of biosynthetic enzymes with each other and the (possible) presence of large biosynthetic complexes (GAGosomes) [48]. This makes the regulation of GAG biosynthesis very complex, gene expression being only a part of it.

Taken together, it is concluded that a highly dynamic expression of genes involved in GAG metabolism and in GAG binding growth factors is associated with skin development. This indicates the importance of fine tuning of GAG structures during developmental processes. Further studies should focus on the biochemical analysis of the GAGs chains themselves.

Data Availability

The EXON array data used to support the findings of this study are included within the article and are provided via [18]. The Taqman low density array data used to support the findings of this study are included within the article. The data used to support the findings of this study are available from the corresponding author upon request.

Conflicts of Interest

The authors declare that they have no conflicts of interest.

Authors' Contributions

P. J. E. Uijtdewilligen wrote the main manuscript text and prepared Figure 1, Tables 1–4, and Supplementary data Tables 1–6. P. J. E. Uijtdewilligen, E. M. Versteeg, and E. M. A. van de Westerlo were responsible for the performance of the genetic analysis using RNA isolation, real time quantitative PCR, and microarray analysis. P. J. E. Uijtdewilligen, J. van der Vlag and T. H. van Kuppevelt were responsible for the design of the Taqman Low Density Array as described in Supplementary data 1-2. W. F. Daamen and T. H. van Kuppevelt were involved in study design, manuscript text, and design of the figures. All authors have given approval for the final version of the manuscript.

Acknowledgments

This study was financially supported by the Dutch Program for Tissue Engineering (DPTE6735). The authors would like to thank the Microarray Facility Nijmegen of the Radboud University Medical Center (The Netherlands) for carrying out the array experiments and assistance with the data analysis. The Central Animal Laboratory of the Radboud University Medical Center is acknowledged for assistance with the animal experiments.

Supplementary Materials

The supplementary data contains 6 tables: Supplemental data Table 1: Design TLDA cart version 1: An overview of the used genes/assays on the Taqman Low Density Array, version 1. This table supports the materials and method section and the results section. Supplemental data Table 2: Design TLDA cart version 2: An overview of the used genes/assays on the Taqman Low Density Array, version 2. This table supports the materials and method section and the results section. Supplemental data Table 3: Deferentially expressed genes as % per category. This table provides a comparison between the EXON array expression data and the TLDA Data Supplemental data Table 4: Deferentially expressed genes during skin development in mice in comparison to mature mouse skin using TLDA cards. Supplemental data Table 5: Differentially expressed genes during skin development in mice in comparison to mature mouse skin using EXON array Supplementary data Table 6: Differentially expressed genes found using Taqman Low Density Arrays for the Glce knockout and HSPEtg mouse compared to wild type. *(Supplementary Materials)*

References

[1] H. E. Bülow and O. Hobert, "The molecular diversity of glycosaminoglycans shapes animal development," *Annual Review of Cell and Developmental Biology*, vol. 22, no. 1, pp. 375–407, 2006.

[2] S. Sarrazin, W. C. Lamanna, and J. D. Esko, "Heparan sulfate proteoglycans," *Cold Spring Harbor Perspectives in Biology*, vol. 3, no. 7, pp. 1–33, 2011.

[3] I. Matsuo and C. Kimura-Yoshida, "Extracellular modulation of fibroblast growth factor signaling through heparan sulfate proteoglycans in mammalian development," *Current Opinion in Genetics & Development*, vol. 23, no. 4, pp. 399–407, 2013.

[4] P. Olczyk, Ł. Mencner, and K. Komosinska-Vassev, "The role of the extracellular matrix components in cutaneous wound healing," *BioMed Research International*, vol. 2014, Article ID 747584, 8 pages, 2014.

[5] M. Maccarana, S. Kalamajski, M. Kongsgaard, S. Peter Magnusson, A. Oldberg, and A. Malmström, "Dermatan sulfate epimerase 1-deficient mice have reduced content and changed distribution of iduronic acids in dermatan sulfate and an altered collagen structure in skin," *Molecular and Cellular Biology*, vol. 29, no. 20, pp. 5517–5528, 2009.

[6] J. K. Mouw, G. Ou, and V. M. Weaver, "Extracellular matrix assembly: a multiscale deconstruction," *Nature Reviews Molecular Cell Biology*, vol. 15, no. 12, pp. 771–785, 2014.

[7] E. Zcharia, S. Metzger, T. Chajek-Shaul et al., "Transgenic expression of mammalian heparanase uncovers physiological functions of heparan sulfate in tissue morphogenesis, vascularization, and feeding behavior," *The FASEB Journal*, vol. 18, no. 2, pp. 252–263, 2004.

[8] V. J. Coulson-Thomas, T. F. Gesteira, J. Esko, and W. Kao, "Heparan sulfate regulates hair follicle and sebaceous gland morphogenesis and homeostasis," *The Journal of Biological Chemistry*, vol. 289, no. 36, pp. 25211–25226, 2014.

[9] E. Zcharia, R. Zilka, A. Yaar et al., "Heparanase accelerates wound angiogenesis and wound healing in mouse and rat models," *The FASEB Journal*, vol. 19, no. 2, pp. 211–221, 2005.

[10] S. Mizumoto, S. Yamada, and K. Sugahara, "Human genetic disorders and knockout mice deficient in glycosaminoglycan," *BioMed Research International*, vol. 2014, Article ID 495764, 24 pages, 2014.

[11] K. Grobe, M. Inatani, S. R. Pallerla, J. Castagnola, Y. Yamaguchi, and J. D. Esko, "Cerebral hypoplasia and craniofacial defects in mice lacking heparan sulfate Ndst1 gene function," *Development*, vol. 132, no. 16, pp. 3777–3786, 2005.

[12] R. M. Witt, M.-L. Hecht, M. F. Pazyra-Murphy et al., "Heparan sulfate proteoglycans containing a glypican 5 core and 2-O-sulfo-iduronic acid function as sonic hedgehog co-receptors to promote proliferation," *The Journal of Biological Chemistry*, vol. 288, no. 36, pp. 26275–26288, 2013.

[13] J.-P. Li, F. Gong, Å. Hagner-McWhirter et al., "Targeted disruption of a murine glucuronyl C5-epimerase gene results in heparan sulfate lacking L-iduronic acid and in neonatal lethality," *The Journal of Biological Chemistry*, vol. 278, no. 31, pp. 28363–28366, 2003.

[14] J. Jia, M. Maccarana, X. Zhang, M. Bespalov, U. Lindahl, and J.-P. Li, "Lack of L-iduronic acid in heparan sulfate affects interaction with growth factors and cell signaling," *The Journal of Biological Chemistry*, vol. 284, no. 23, pp. 15942–15950, 2009.

[15] H. Habuchi, N. Nagai, N. Sugaya, F. Atsumi, R. L. Stevens, and K. Kimata, "Mice deficient in heparan sulfate 6-O-sulfotransferase-1 exhibit defective heparan sulfate biosynthesis, abnormal placentation, and late embryonic lethality," *The Journal of Biological Chemistry*, vol. 282, no. 21, pp. 15578–15588, 2007.

[16] M. Tong, B. Tuk, I. M. Hekking, M. Vermeij, D. Barritault, and J. W. Van Neck, "Stimulated neovascularization, inflammation resolution and collagen maturation in healing rat cutaneous wounds by a heparan sulfate glycosaminoglycan mimetic, OTR4120," *Wound Repair and Regeneration*, vol. 17, no. 6, pp. 840–852, 2009.

[17] D. Barritault, M. Gilbert-Sirieix, K. L. Rice et al., "RGTA® or ReGeneraTing Agents mimic heparan sulfate in regenerative medicine: from concept to curing patients," *Glycoconjugate Journal*, vol. 34, no. 3, pp. 325–338, 2017.

[18] P. J. E. Uijtdewilligen, E. M. M. Versteeg, C. Gilissen et al., "Towards embryonic-like scaffolds for skin tissue engineering: Identification of effector molecules and construction of scaffolds," *Journal of Tissue Engineering and Regenerative Medicine*, vol. 10, no. 1, pp. E34–E44, 2016.

[19] J. Rossant and P. P. L. Tam, *Mouse Development: Patterning, Morphogenesis, and Organogenesis*, Academic Press, London, UK, 2002.

[20] J.-P. Li, F. Gong, K. El Darwish, M. Jalkanen, and U. Lindahl, "Characterization of the D-Glucuronyl C5-epimerase Involved in the Biosynthesis of Heparin and Heparan Sulfate," *The Journal of Biological Chemistry*, vol. 276, no. 23, pp. 20069–20077, 2001.

[21] K. Kadota and K. Shimizu, "Evaluating methods for ranking differentially expressed genes applied to microArray quality control data," *BMC Bioinformatics*, vol. 12, no. 1, p. 227, 2011.

[22] G. Lammers, C. Gilissen, S. T. M. Nillesen et al., "High density gene expression microarrays and gene ontology analysis for identifying processes in implanted tissue engineering constructs," *Biomaterials*, vol. 31, no. 32, pp. 8299–8312, 2010.

[23] K. J. Livak and T. D. Schmittgen, "Analysis of relative gene expression data using real-time quantitative PCR and the $2^{-\Delta\Delta CT}$ method," *Methods*, vol. 25, no. 4, pp. 402–408, 2001.

[24] Y. Benjamini and Y. Hochberg, "Controlling the false discovery rate: a practical and powerful approach to multiple testing," *Journal of the Royal Statistical Society B: Methodological*, vol. 57, no. 1, pp. 289–300, 1995.

[25] H. H. Song and J. Filmus, "The role of glypicans in mammalian development," *Biochimica et Biophysica Acta (BBA) - General Subjects*, vol. 1573, no. 3, pp. 241–246, 2002.

[26] J. Filmus and M. Capurro, "The role of glypicans in Hedgehog signaling," *Matrix Biology*, vol. 35, pp. 248–252, 2014.

[27] M. Buono, I. Visigalli, R. Bergamasco, A. Biffi, and M. P. Cosma, "Sulfatase modifying factor 1-mediated fibroblast growth factor signaling primes hematopoietic multilineage development," *The Journal of Experimental Medicine*, vol. 207, no. 8, pp. 1647–1660, 2010.

[28] D. Yan and X. Lin, "Shaping morphogen gradients by proteoglycans," *Cold Spring Harbor Perspectives in Biology*, vol. 1, no. 3, pp. 1–17, 2009.

[29] A. B. Campos-Xavier, D. Martinet, J. Bateman et al., "Mutations in the Heparan-Sulfate Proteoglycan Glypican 6 (GPC6) Impair Endochondral Ossification and Cause Recessive Omodysplasia," *American Journal of Human Genetics*, vol. 84, no. 6, pp. 760–770, 2009.

[30] E. Chiao, P. Fisher, L. Crisponi et al., "Overgrowth of a mouse model of the Simpson - Golabi - Behmel syndrome is independent of IGF signaling," *Developmental Biology*, vol. 243, no. 1, pp. 185–206, 2002.

[31] M. I. Capurro, P. Xu, W. Shi, F. Li, A. Jia, and J. Filmus, "Glypican-3 Inhibits Hedgehog Signaling during Development by Competing with Patched for Hedgehog Binding," *Developmental Cell*, vol. 14, no. 5, pp. 700–711, 2008.

[32] A. E. Oro and K. Higgins, "Hair cycle regulation of Hedgehog signal reception," *Developmental Biology*, vol. 255, no. 2, pp. 238–248, 2003.

[33] F. X. Maquart and J. C. Monboisse, "Extracellular matrix and wound healing," *Pathologie Biologie*, vol. 62, no. 2, pp. 91–95, 2014.

[34] G. D. Richardson, K. A. Fantauzzo, H. Bazzi, A. Määttä, and C. A. B. Jahoda, "Dynamic expression of Syndecan-1 during hair follicle morphogenesis," *Gene Expression Patterns*, vol. 9, no. 6, pp. 454–460, 2009.

[35] S. Nadanaka, S. Zhou, S. Kagiyama et al., "EXTL2, a member of the EXT family of tumor suppressors, controls glycosaminoglycan biosynthesis in a xylose kinase-dependent manner," *The Journal of Biological Chemistry*, vol. 288, no. 13, pp. 9321–9333, 2013.

[36] B.-T. Kim, H. Kitagawa, J.-I. Tamura et al., "Human tumor suppressor EXT gene family members EXTL1 and EXTL3 encode α1,4-N-acetylglucosaminyltransferases that likely are involved in heparan sulfate/heparin biosynthesis," *Proceedings of the National Acadamy of Sciences of the United States of America*, vol. 98, no. 13, pp. 7176–7181, 2001.

[37] T. Sato, M. Gotoh, K. Kiyohara et al., "Differential roles of two N-acetylgalactosaminyltransferases, CSGalNAcT-1, and a novel enzyme, CSGalNAcT-2. Initiation and elongation in synthesis of chondroitin sulfate," *The Journal of Biological Chemistry*, vol. 278, no. 5, pp. 3063–3071, 2003.

[38] A. Varki, R. D. Cummings, J. Esko et al., Essentials of Glycobiology, 1999.

[39] J.-I. Aikawa, K. Grobe, M. Tsujimoto, and J. D. Esko, "Multiple isozymes of heparan sulfate/heparin GlcNAc N-deacetylase/GlcN N-sulfotransferase. Structure and activity of

the fourth member, NDST4," *The Journal of Biological Chemistry*, vol. 276, no. 8, pp. 5876–5882, 2001.

[40] T. H. van Kuppevelt, M. A. Dennisseni, W. J. van Venrooij, R. M. A. Hoet, and J. H. Veerkamp, "Generation and application of type-specific anti-heparan sulfate antibodies using phage display technology: further evidence for heparan sulfate heterogeneity in the kidney," *The Journal of Biological Chemistry*, vol. 273, no. 21, pp. 12960–12966, 1998.

[41] H. Habuchi and K. Kimata, "Mice Deficient in Heparan Sulfate 6-O-Sulfotransferase-1," *Progress in Molecular Biology and Translational Science*, vol. 93, pp. 79–111, 2010.

[42] S. Malgouries, M. Donovan, S. Thibaut, and B. A. Bernard, "Heparanase 1: A key participant of inner root sheath differentiation program and hair follicle homeostasis," *Experimental Dermatology*, vol. 17, no. 12, pp. 1017–1023, 2008.

[43] V. N. Patel, S. M. Knox, K. M. Likar et al., "Heparanase cleavage of perlecan heparan sulfate modulates FGF10 activity during ex vivo submandibular gland branching morphogenesis," *Development*, vol. 134, no. 23, pp. 4177–4186, 2007.

[44] R. B. Widelitz, "Wnt signaling in skin organogenesis," *Organogenesis*, vol. 4, no. 2, pp. 123–133, 2008.

[45] L. Créancier, D. Morello, P. Mercier, and A.-C. Prats, "Fibroblast growth factor 2 internal ribosome entry site (IRES) activity ex vivo and in transgenic mice reveals a stringent tissue-specific regulation," *The Journal of Cell Biology*, vol. 150, no. 1, pp. 275–281, 2000.

[46] K. Grobe and J. D. Esko, "Regulated translation of heparan sulfate N-acetylglucosamine N-deacetylase/N-sulfotransferase isozymes by structured 5′-untranslated regions and internal ribosome entry sites," *The Journal of Biological Chemistry*, vol. 277, no. 34, pp. 30699–30706, 2002.

[47] C. U. T. Hellen and P. Sarnow, "Internal ribosome entry sites in eukaryotic mRNA molecules," *Genes & Development*, vol. 15, no. 13, pp. 1593–1612, 2001.

[48] J. D. Esko and S. B. Selleck, "Order out of chaos: assembly of ligand binding sites in heparan sulfate," *Annual Review of Biochemistry*, vol. 71, pp. 435–471, 2002.